

Helimagnetism and weak ferromagnetism in NaCu_2O_2 and related frustrated chain cuprates

This article has been downloaded from IOPscience. Please scroll down to see the full text article.

2007 J. Phys.: Condens. Matter 19 145230

(<http://iopscience.iop.org/0953-8984/19/14/145230>)

View [the table of contents for this issue](#), or go to the [journal homepage](#) for more

Download details:

IP Address: 129.252.86.83

The article was downloaded on 28/05/2010 at 17:28

Please note that [terms and conditions apply](#).

Helimagnetism and weak ferromagnetism in NaCu_2O_2 and related frustrated chain cuprates

S-L Drechsler¹, N Tristan¹, R Klingeler¹, B Büchner¹, J Richter²,
J Málek³, O Volkova^{4,6}, A Vasiliev⁴, M Schmitt⁵, A Ormeci⁵, C Loison⁵,
W Schnelle⁵ and H Rosner⁵

¹ Leibniz-Institut für Festkörper- und Werkstoffforschung IFW Dresden, PO Box 270116,
Dresden D-01171, Germany

² Inst. f. Theor. Phys., Universität Magdeburg, Magdeburg D-39016, Germany

³ Institute of Physics, ASCR, Prague, Czech Republic

⁴ Moscow State University, 119992 Moscow, Russia

⁵ Max-Planck-Institut f. chem. Physik fester Stoffe, Dresden D-01187, Germany

⁶ Institute of Radiotechnics and Electronics, RAS, Moscow 125009, Russia

E-mail: s.l.drechsler@ifw-dresden.de

Received 8 September 2006

Published 23 March 2007

Online at stacks.iop.org/JPhysCM/19/145230

Abstract

A novel subclass of frustrated undoped edge-shared CuO_2 chain materials with intriguing magnetism is briefly reviewed. These cuprates show at low temperature a tendency to helicoidal magnetic ordering with acute pitches and in some cases also to weak ferromagnetism. In our analysis we focus on our recent theoretical and experimental studies on $\text{Na}(\text{Li})\text{Cu}_2\text{O}_2$ and related systems. Differences and similarities in the magnetic ground states of these structurally similar localized spin-1/2 compounds are considered. The nontrivial interplay of frustrated single-chain couplings, anisotropy and interchain exchange is stressed.

(Some figures in this article are in colour only in the electronic version)

1. Introduction—a brief history of magnetism in edge-shared chain cuprates

Even undoped edge-shared (ES) CuO_2 chain systems (see e.g. figure 1) exhibit a large variety of magnetic ground states. Thus, below $T_N \approx 9$ K the archetype Li_2CuO_2 [1] shows a Néel state caused by antiferromagnetic (AFM) interchain coupling and a ferromagnetic (FM) in-chain ordering. In contrast, the closely related LiVCuO_4 [2, 3], LiCu_2O_2 [4–8], and NaCu_2O_2 [9–11] show incommensurate magnetic structures (ICMSs) along the chain direction b below $T_h \approx 3$, 24, and 13 K, respectively. These structures represent the first long sought [12] helices with acute pitches for localized quantum spin ($s = 1/2$) chain systems. At first, guided by maxima in the magnetic susceptibility $\chi(T)$ and the specific heat c_p at relatively low T , nearly ideal

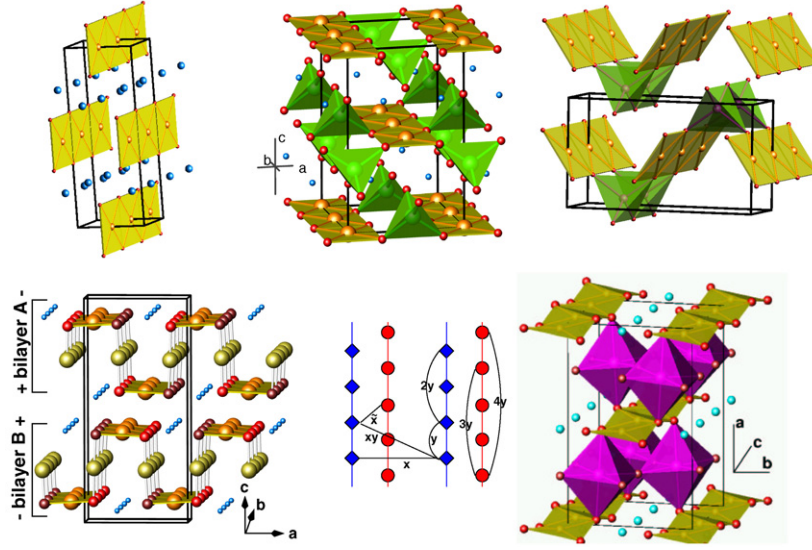


Figure 1. Structure of ES chain cuprates. Upper row: planar CuO_2 chains $\parallel b$ for Li_2CuO_2 (left), LiCuVO_4 (middle), and CuGeO_3 (right). Notation: big orange O — Cu^{2+} , small red O — O , big green O — V or Ge , and small blue O — Li . Lower row: buckled chains. The formally double-chain (DC) systems $\text{Na}(\text{Li})\text{Cu}_2\text{O}_2$ with a DC in the centre (left), notation as above; big yellow O —the Cu^+ ions, nonequivalent O in small red and brown O . Projected bi-layer onto the $(a, b) \equiv (x, y)$ plane with two DCs (middle). \blacklozenge and \bullet denote Cu in different planes. The main exchange paths are given by arches ($y = J_1, 2y = J_2$, etc, $\bar{x} = \bar{J}$). Right: $\text{Li}_2\text{ZrCuO}_4$ with buckled chains $\parallel c$. Notation as above, but Cu —bright olive-green O , Zr —bright O inside the magenta corner-shared ZrO_6 octahedra.

1D-AFM Heisenberg behaviour with a Néel ordering at $T \rightarrow 0$ due to residual 3D couplings was suggested [13–18]. The magnetic properties can be described by the Hamiltonian

$$\mathcal{H} = \sum_{ij, \alpha\beta} J_{ij}^{\alpha\beta} S_i^\alpha S_j^\beta + \mathbf{D}_{ij} \cdot (\mathbf{S}_i \times \mathbf{S}_j), \quad (1)$$

where i, j run over pairs of nearest neighbour (NN), next nearest neighbour (NNN), etc CuO_4 plaquettes. The second antisymmetric exchange term (Dzyaloshinskii–Moryia (DM)) is allowed by symmetry only for certain nonideal chains. \mathcal{H} applied to a real chain system shows an exchange hierarchy with the leading isotropic NN and NNN in-chain exchange denoted below as J_1 and J_2 , respectively. Then symmetric exchange anisotropy [15–18] and the possibility of helical ICMS ground states was realized. By neutron diffraction (ND) for LiCuVO_4 and $\text{Na}(\text{Li})\text{Cu}_2\text{O}_2$ [2–4, 9] the corresponding propagation vectors, $\zeta = 0.234, 0.227$, and 0.1724 , respectively (in units of $2\pi/b$ for a single chain), have been found. The related pitches read $\phi = 84.2(83.6 \pm 0.6)^\circ, 81.7^\circ, 62.1^\circ$. However, the acute ϕ assignment from ND alone is not unique [19]⁷. A detailed analysis of e.g. inelastic neutron scattering (INS) [3, 22] and $\chi(T)$ data [5–7, 9, 10] is necessary to settle unambiguously that the sign of J_1 is FM, i.e. $J_1 < 0$. In $\text{Na}(\text{Li})\text{Cu}_2\text{O}_2$ a significant AFM double-chain (DC) exchange \bar{J} (figure 1) might affect the ICMS. For LiCu_2O_2 two alternative models have been employed to interpret the data: (i) the ‘AFM–AFM’ DC (AADC) [4, 20, 21] and (ii) the isotropic FM–AFM single-chain J_1 – J_2 model (FASCJ1J2) [5–7]. In the meantime the validity of model (ii) as a good starting point

⁷ The sets symmetric to $1/4, \zeta' = 1/2 - \zeta$, lead to obtuse pitches $\phi' = 95.8$ (96.4) $^\circ$, etc; i.e. AFM J_1 values would also fit the data.

has been accepted [8, 22], supported also by new data for the isomorphous NaCu_2O_2 [9–11], except recent ARPES (angle resolved photoemission) data for LiCu_2O_2 [23] by Papagno *et al*, who analysed it within an *unfrustrated* 1D spinon–holon picture. But its microscopic meaning remains unclear (see below). For NaCu_2O_2 a slight extension of model (ii), a frustrated FM–AFM–AFM–AFM J_1 – J_4 model with two added AFM long-range couplings J_3 and J_4 , has been proposed [9] (figure 1). Finally, using low- T fits of $\chi(T)$ Hase *et al* [24] also applied model (ii) to $\text{Rb}(\text{Cs})_2\text{Cu}_2\text{Mo}_3\text{O}_{12}$. Above 2 K no ordering could be found for these two systems. For linearite ($\text{Pb}[\text{Cu}(\text{SO}_4)(\text{OH})_2]$) some ordering occurs at $T \approx 2.7$ K [26].

2. Basic electronic structure and the microscopic origin of the frustration

The above mentioned disparity in T_h , pitches, the possible subsequent occurrence of weak ferromagnetism at $T^* \leq T_h$, or disorder at low T results from a complex interplay between the strength of frustration, the anisotropy of in-chain and perpendicular transfer integrals governed by the Cu–O–Cu bond angle $\gamma \sim 90^\circ$, the exchange anisotropy affected by local distortions from the ideal flat chain geometry, the strength of the crystal field affected by the position and the charge of the cations, as well as the interchain exchange. $\text{Rb}(\text{Cs})_2\text{Cu}_2\text{Mo}_3\text{O}_{12}$ show⁸ strongly distorted nonplanar chains formed by an unusual asymmetric (nondiagonal!) corner-sharing of NN CuO_4 plaquettes with a Cu–O–Cu $\gamma = 103^\circ$. The arrangement of NNN plaquettes resembles that in ES CuO_2 chains, which points to an AFM J_2 , whereas the FM nature of J_1 is similar to that of the strongly buckled rungs in the pseudo-ladder compound MgCu_2O_3 with a Cu–O–Cu of 108° [27]. Noteworthily, the commonly used chemical notation is somewhat misleading because it does not reflect properly the cuprate character, which however dominates the low-energy electronic and magnetic properties. For instance, according to the orbital analysis of states near the Fermi energy E_F using the FPLO-LDA band structure code [28], transition-metal-ion-derived states, except Cu^{2+} , do enter mainly magnetically inert complex cations to compensate the anionic cuprate units (see figure 2, lower panel). Thus, $\text{Li}_2\text{ZrCuO}_4$ (LiCuVO_4) (figure 1) is not a zirconate (vanadate), but a Li zirconyl (vanadyl) cuprate, more correctly written as $[\text{Li}_2\text{ZrO}_2]^{2+}[\text{CuO}_2]^{2-}$ or $[\text{LiVO}_2]^{2+}[\text{CuO}_2]^{2-}$. Here Zr and V are almost in Zr^{4+} or V^{5+} states with empty 4d and 5s or 3d and 4s shells and therefore they are magnetically silent, similar to Mo^{6+} in $\text{Rb}(\text{Cs})_2\text{Cu}_2\text{Mo}_3\text{O}_{12}$. In $\text{Li}(\text{Na})\text{Cu}_2\text{O}_2$ there are two Cu sites: one Cu^{2+} in the chains is magnetically active whereas Cu^+ in between (see figure 1) is non-magnetic. Finally, Pb^{4+} enters linearite with a filled 5d shell. From the strong correlation for Cu^{2+} systems it follows that all undoped ES chain cuprates are charge transfer (CT) insulators with corresponding large CT gap values of the order of $\Delta_{\text{pd}} \sim 3$ –4 eV or even larger. However, the observed smaller optical gap $E_g \approx 1.95$ eV in LiCu_2O_2 [23] (although comparable with that in the 2D corner-shared La_2CuO_4) must be of another origin because here the generically restricted hole mobility due to the nearly 90° NN Cu–O–Cu bond angle leads to a larger CT gap. Unlike the CT-gap assignment given in [23], the observed small E_g results probably from transitions into an empty Cu 4s derived band inside the CT gap. The large holon and spinon dispersions of $2t_{\text{eff}} \approx 0.74$ eV and $0.5\pi J_{\text{eff}} \approx 55$ meV, respectively, found there contradict the small width of the half-filled band at E_F (figure 2). Within the LDA it is for all ES chains only ~ 0.5 – 0.8 eV. Further difficulties arise from a simple internal self-consistency check⁹. If one takes into account only NN and NNN exchange, for AFM

⁸ We note that the J -values for $\text{Rb}(\text{Cs})_2\text{Cu}_2\text{Mo}_3\text{O}_{12}$ have been slightly changed compared with the values of low- T χ fits [24]. We also used the reported FM Θ_{CW} and adopted a weak interchain exchange of ~ 1 meV with two NN chains.

⁹ Adopting a typical value for the effective *one-band* (!) Hubbard $U \sim 3$ –4 eV instead of the $U_{dd} \sim 8$ eV (appropriate only for an O 2p Cu 3d five-band model) used in [23], one would arrive at $J_{\text{eff}} = 4t_{\text{eff}}^2/U \geq 136$ meV, which exceeds greatly the ARPES-based estimate of 35 meV and $J_1 \sim 15$ meV for the strongest AFM ES CuO_2 system CuGeO_3 .

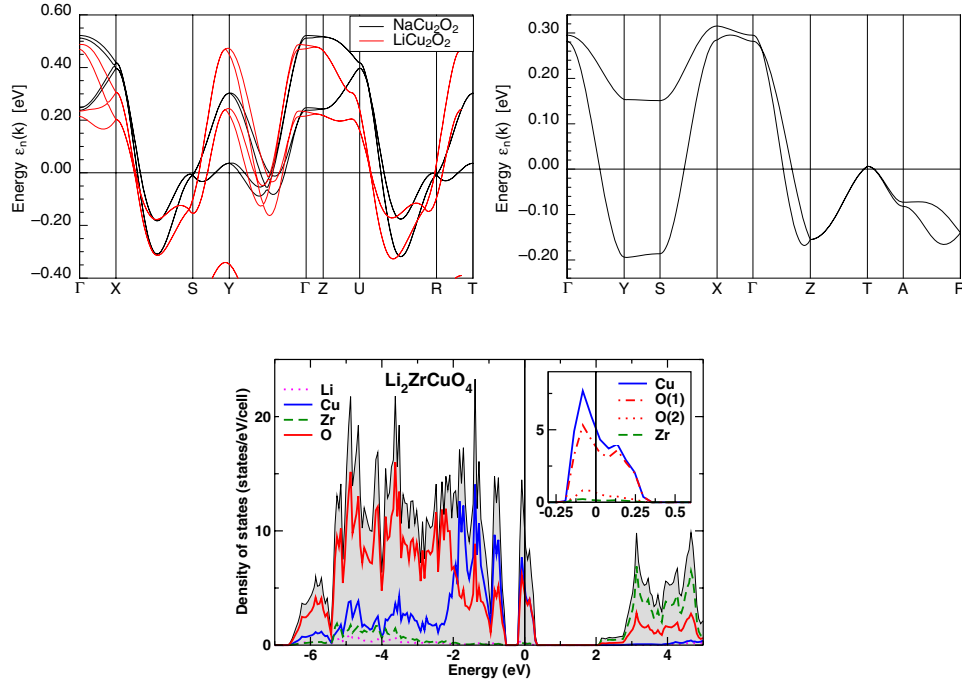


Figure 2. Comparison of LDA-FPLO band structures for the isomorphic DC systems ACu_2O_2 , $\text{A} = \text{Li, Na}$ (upper left panel), $\text{Li}_2\text{ZrCuO}_4$ (upper right panel), and the atomic orbital resolved density of states for the latter system (lower panel). Γ, X, Y, Z, \dots is the standard wavevector notation for symmetry points $(0, 0, 0); (2\pi/a, 0, 0); (0, 2\pi/b, 0); (0, 0, 2\pi/c); \dots$, respectively.

NNN coupling along a single CuO_2 chain a frustration problem arises for any sign of J_1 . In the following the frustration is measured by the ratio $\alpha = -J_2/J_1$. Although the considered systems exhibit rather different FM NN values, i.e. $J_1 = -1.8$ to -40 meV, the AFM NNN counterpart differs less: $J_2 = 7.5 \pm 3.5$ meV has been derived from $\chi(T)$ and $c_p(T)$ fits as well as from the LDA-FPLO 3D band structure and total energies of various simple constraint magnetic superstructures within the LSDA + U [29] or directly by calculating the exchange related unscreened Coulomb matrix elements using one-band Wannier functions [3, 5, 10]. For the well studied Li_2CuO_2 , we fitted an extended five-band Hubbard model to describe the optical conductivity and the O 1s x-ray absorption [30]. Then the low-energy states of Cu_nO_{2n} rings with $n = 3-6$ have been mapped onto the corresponding rings of a J_1 - J_2 -Heisenberg model. Due to a non-negligible NNN transfer integral t_{2y} , the analysis yields $\alpha \approx 0.7$, which exceeds the well known critical value of $\alpha_c^{\text{1D}} = 1/4$ for a spiral instability. This seeming conflict with ND data showing a FM in-chain ordering can be resolved by the specific interchain exchange in Li_2CuO_2 [6, 12]. In contrast, the interchain exchange only weakly affects α_c in LiVCuO_4 and $\text{Na(Li)Cu}_2\text{O}_2$.

3. Thermodynamic properties and weak ferromagnetism

Analysis of $\chi(T)$, $M(T, H)$, and $c_p(T)$ data provide insight into the main exchange. For example, the shape of $\chi(T)$ and its Curie-Weiss temperature Θ_{CW} yield constraints for α and the interchain exchange. Typical shapes of $\chi(T)$ together with fits by the FASCJ1J2 model

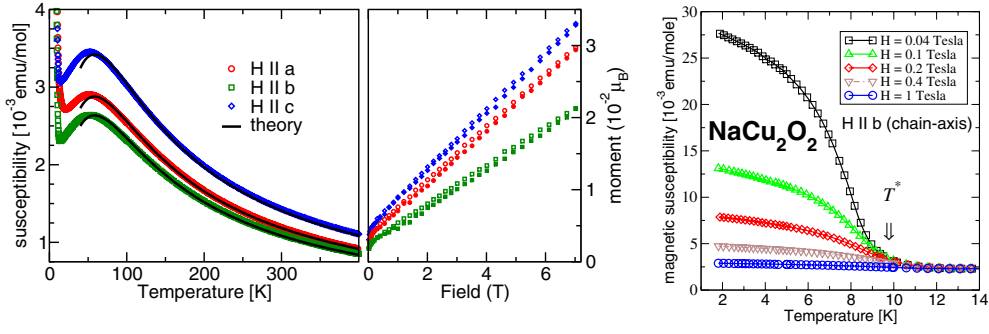


Figure 3. Magnetic susceptibilities $\chi(T)$ for spin-1/2 FM–AFM J_1 – J_2 Heisenberg rings with $N = 16$ sites compared with experimental data for NaCu_2O_2 [10] (left). Magnetization versus applied field at $T = 2$ K (middle). Low- T spin susceptibility $\chi(T)$ for different magnetic fields H applied in the chain direction (right). T^* denotes the onset of the weak ferromagnetism.

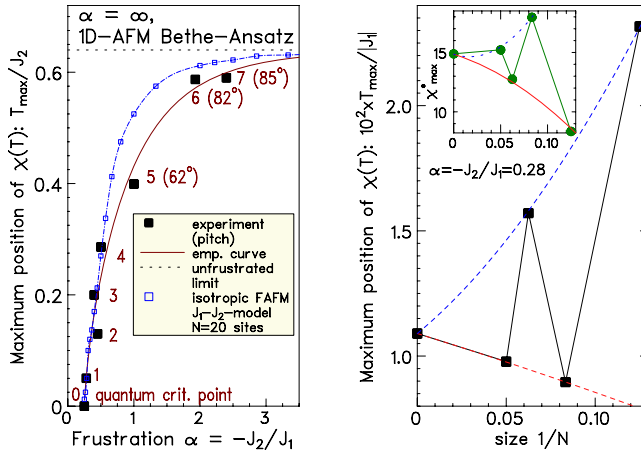


Figure 4. Temperature of the maximum of $\chi(T)$ in units of estimated NNN exchange integrals J_2 of the FASCJ1J2-model versus the frustration ratio $\alpha = -J_2/J_1$ for various ES chain cuprates: 1— $\text{Li}_2\text{ZrCuO}_4$, 2—linearite, 3— $\text{Rb}_2\text{Cu}_2\text{Mo}_3\text{O}_{12}$, 4— $\text{Cs}_2\text{Cu}_2\text{Mo}_3\text{O}_{12}$, 5— Li_2CuO_2 , 6— Na_2CuO_2 , and 7— LiCuVO_4 (left). Finite size analysis for $1, N = \infty$ data from TMRG [32], $\chi^* = \chi|J_1|/g^2\mu_B^2$ (right).

for NaCu_2O_2 are shown in figure 3. A downshift of the empirical maximum positions $T_{\text{max}}^X/J_2 \rightarrow \alpha_c$ of the same model applied to related systems is shown in figure 4. Our analysis of $\chi(T)$ and c_p for $\text{Li}_2\text{ZrCuO}_4$ taken from [25] yields $\alpha \approx 0.28$ – 0.3 , i.e. close to the quantum critical point $\alpha_c = 1/4$ (the spiral-FM transition). In figure 4 the predicted T_{max}^X/J_2 within the FASCJ1J2-model is shown, too, as derived from full diagonalizations of rings with $N = 20$ sites using our own and their results [31, 32] (transfer matrix renormalization group (TMRG)). Despite small corrections due to finite N , exchange anisotropy, and doped holes (from stoichiometry deviations in real systems), based on the consistent picture we may conclude that the considered systems in fact belong to a novel subclass of ES chain cuprates different from the ‘FM’ Li_2CuO_2 and the AFM–AFM spin–Peierls system CuGeO_3 .

The staggered tilting of CuO_4 plaquettes of all four nonplanar chain compounds $\text{Li}_2\text{ZrCuO}_4$, $\text{Pb}_2[\text{CuSO}_4(\text{OH})_2]$, and $\text{Rb}(\text{Cs})_2\text{Cu}_2\text{Mo}_3\text{O}_{12}$ as well as within the bilayers of $\text{Na}(\text{Li})\text{Cu}_2\text{O}_2$ along a may cause oscillating terms in \mathcal{H} , i.e. a staggered field induced

magnetization which yields a spin gap Δ_s for one of the two acoustic branches near Γ , akin to the mechanism proposed for Cu benzoate at the 1D Brillouin zone (BZ) boundary [33]. An H dependent Δ_s could explain the field sensitivity of T_h at moderate H seen in Na_2CuO_2 .

Another notable point is the hysteresis at $H < 1$ T in NaCu_2O_2 below $T^* \approx 9$ K, well below $T_h = 13$ K (figure 3). The observed local moment $M_0 \approx 4 \times 10^{-3} \mu_B$ at $T = 2$ K is comparable with that of other weak FM cuprates. Usually, weak ferromagnetism is ascribed to DM exchange allowed in $\text{NaCu}_2\text{CuO}_2$ by the low local symmetry. In fact, the inspection of the slightly tilted CuO_4 plaquettes reveals a shift of the Cu^{2+} ions off from their centre (figure 1), which might explain the origin of DM¹⁰. Alternatively, it might also be regarded as a secondary order parameter induced by the increasing basic spiral one with decreasing T . Thus, the strong enough local magnetic moments induced by the spiral formation finally visualize the broken inversion symmetry of a single chain at $T < T^* < T_h$ and allow the smooth occurrence of significant DM exchange and weak FM only below T^* . Then the suppression of M_0 at moderate fields points to a strong field dependence of the underlying basic magnetic structure. Finally, note that a symmetric exchange anisotropy can also explain the spiral orientation. According to [34] for $\alpha \gg 1$ (only \approx valid here), chiral structures can coexist with ferromagnetism. This might be of relevance for the missing or tiny induced FM moment $M_0 \sim 10^{-5} \mu_B$ in LiCu_2O_2 , which shows $\alpha \approx 1$, only [5–7]. Some details of the spiral, especially its evolution under external magnetic fields, are still unclear. Related problems including possible collinear commensurate quantum phases [35, 36] are briefly discussed in [37].

To conclude, we have shown that the isotropic frustrated FASCJ1J2 model supplemented with realistic interchain exchange and small exchange anisotropies to explain the weak ferromagnetism reveals a proper description at low magnetic fields of various edge-shared CuO_2 chain systems. Li_2CuO_2 is found to be very close to an FM–AFM helical ground state still prevented by a strong specific, frustrated interchain coupling, whereas the long sought ‘FM’ spin-1/2 helix with acute pitches is realized in LiCuVO_4 and $\text{Li}(\text{Na})\text{Cu}_2\text{O}_2$ and possibly also in linearite. For $\text{Rb}(\text{Cs})_2\text{Cu}_2\text{Mo}_3\text{O}_{12}$ a finite T_h strongly suppressed by the frustrating AFM interchain exchange might still be observed at very low T .

Acknowledgments

We thank the DFG (JM, JR, BB, NT, RK and HR (E. Noether programme, grants CRDF RU-P1-2599-MO-04, RFBR 06-02-16088 (OV, AV))) and GIF (HR) for funding.

Note added in proof. In a recent paper by T Hamasaki, H Kuro, T Sekine, T Naka, M Hase, N Maeshima, Y Saiga, and Y Uwatoka, *J. Magn. Magn. Mater.* (at press) (*Proc. Int. Conf. on Magnetism (ICM2006) August 20–25, 2006, Kyoto, Japan*) devoted to the pressure effect on $\text{Rb}(\text{Cs})\text{Cu}_2\text{Mo}_3\text{O}_{12}$ (compounds 3 and 4 in figure 4), the authors report a new fit below 50 K of $\chi(T)$ data for $\text{Rb}_2\text{Cu}_2\text{Mo}_3\text{O}_{12}$ given in [24]. Applying the transfer matrix renormalization group technique to the isotropic FASC J_1 – J_2 Heisenberg model, they arrive at a significantly enhanced J_1 value of -600 K compared with -138 K reported in [24] and at $\alpha = 0.296$, now close to the ferromagnetic critical point $\alpha = 0.25$. For the related $\text{Cs}_2\text{Cu}_2\text{Mo}_3\text{O}_{12}$ compound they found that the isotropic FASC J_1 – J_2 model did not fit the $\chi(T)$ data. Hence, possibly the fit by this model is not unique and the analysis of other quantities like the specific heat $c_p(T, H)$ could be helpful to resolve these puzzles.

References

- [1] Ebisu S *et al* 1998 *J. Phys. Chem. Solids* **59** 1407
- [2] Gibson B J *et al* 2004 *Physica B* **350** e253

¹⁰ Using the fitted g_c and J_1 and J_2 , we estimate the NN DM vector as $|\mathbf{D}_1| = (\Delta g_c/g)|J_1| \sim 0.5$ meV and $|\mathbf{D}_2| = 0.89$ meV for the NNN one.

- [3] Enderle M *et al* 2005 *Europhys. Lett.* **70** 237
- [4] Masuda T *et al* 2004 *Phys. Rev. Lett.* **92** 177201
- [5] Gippius A A *et al* 2004 *Phys. Rev. B* **70** R01426
Gippius A A *et al* 2006 *J. Magn. Magn. Mater.* **300** e335
- [6] Drechsler S-L *et al* 2005 *Phys. Rev. Lett.* **94** 039705
- [7] Drechsler S-L 2005 *J. Magn. Magn. Mater.* **290** 345
- [8] Mihaly M *et al* 2006 *Preprint cond-mat/0601701*
- [9] Capogna L *et al* 2005 *Phys. Rev. B* **71** R140402
- [10] Drechsler S-L *et al* 2006 *Europhys. Lett.* **73** 83
- [11] Choi K-Y *et al* 2006 *Phys. Rev. B* **73** 094409
- [12] Mizuno Y *et al* 1998 *Phys. Rev. B* **57** 5326
- [13] Yamaguchi M *et al* 1996 *J. Phys. Soc. Japan* **65** 2998
- [14] Vasil'ev A N *et al* 2001 *Phys. Rev. B* **64** 024419
- [15] Kegler Ch *et al* 2001 *J. Eur. Phys. B* **22** 321
- [16] Krug von Nidda H-A *et al* 2003 *Phys. Rev. B* **65** 134445
- [17] Maeda Y *et al* 2005 *Phys. Rev. Lett.* **95** 037602
- [18] Kegler Ch *et al* 2006 *Phys. Rev. B* **73** 104418
- [19] Dai D *et al* 2004 *Inorg. Chem.* **43** 4026
- [20] Zvyagin S *et al* 2000 *Phys. Rev. B* **66** 064424
- [21] Choi K-Y *et al* 2004 *Phys. Rev. B* **69** 104421
- [22] Masuda T *et al* 2005 *Phys. Rev. Lett.* **94** 039706
Masuda T *et al* 2005 *Phys. Rev. B* **72** 014405
- [23] Papagno M *et al* 2006 *Phys. Rev. B* **73** 115120
- [24] Hase M *et al* 2005 *Phys. Rev. B* **70** 10426
Hase M *et al* 2005 *J. Appl. Phys. Lett.* **97** 10B303
- [25] Volkova O *et al* 2006 at press
- [26] Baran M *et al* 2006 *Phys. Status Solidi c* **3** 220
- [27] Drechsler S-L *et al* 2004 *Physica C* **408** 270
- [28] Koepernik K and Eschrig H H 1999 *Phys. Rev. B* **59** 1743
- [29] Nitzsche U *et al* 2007 *Physica C* at press
- [30] Neudert R *et al* 1999 *Phys. Rev. B* **60** 13413
- [31] Heidrich-Meisner F *et al* 2006 *Phys. Rev. B* **74** R020403
- [32] Lu H T *et al* 2006 *Preprint cond-mat/0603519*
- [33] Oshikawa M and Affleck I 1997 *Phys. Rev. Lett.* **79** 2886
- [34] Zarea Z *et al* 2004 *Eur. J. Phys. B* **39** 1434
- [35] Dmitriev D and Krivnov V 2006 *Phys. Rev. B* **73** 024402
- [36] Kuzian R and Drechsler S-L 2006 *Phys. Rev. B* submitted
- [37] Drechsler S-L *et al* 2006 *J. Magn. Magn. Mater.* submitted